JOURNAL OF MATERIALS SCIENCE **32** (1997) 4931–4940

# Wettability of NiAl by a liquid Ni–Si–B alloy

W.F. GALE, J.W. FERGUS, W.M. INGRAM
*Materials Research and Education Center, Auburn University, Auburn, AL 36849, USA*
M. KOOPMAN
*Department of Materials Science, University of Alabama in Birmingham, Birmingham, AL 35294, USA*

An investigation of the wettability of the intermetallic compound NiAl by a liquid Ni–4.5 wt% Si–3.2 wt% B filler metal is presented in this paper. Dynamic observations of spreading of Ni–Si–B droplets, conducted using hot-stage light microscopy, are correlated with post-cooling microscopy and analysis. The paper examines the influence of the oxide layer on the NiAl substrates, on the progression of spreading of the Ni–Si–B liquid. Termination of spreading of the Ni–Si–B droplets by the onset of isothermal solidification at the spreading front is considered.

Spreading of the Ni–Si–B droplets was found to be rapid until the onset of isothermal solidification at the spreading front. However, once isothermal solidification commenced, negligible further spreading was observed. The Ni–Si–B filler metal was observed to spread by undermining of the substrate oxide. However, a marked reaction occurred between the substrate oxide and the Ni–Si–B filler metal. This reaction served to remove the substrate oxide layer. The paper contrasts the mechanisms of substrate oxide undermining and isothermal solidification of liquid Ni–Si–B droplets on NiAl with those occurring during the spreading of the same liquid on pure nickel and Ni–Cr alloys.

## 1. Introduction

The intermetallic compound NiAl [1–5] has attracted considerable interest as a structural material for elevated-temperature service [6]. If NiAl is to find large-scale practical applications, then joining technologies will be required [6], for both initial fabrication and post-service repair. The transient liquid phase (TLP) bonding process [7] offers compatibility with the poor low-temperature ductility [8] and strong alumina-forming tendency of NiAl [9].

Microstructural development during TLP bonding of NiAl–NiAl and NiAl–Ni has formed the subject of a number of investigations [10–13]. However, similar attention has not been paid to the wettability of NiAl during TLP bonding. Wettability of the substrates by the interlayer material is a prerequisite for successful TLP bonding. Thus, the present paper examines the spreading of liquid Ni–4.5 wt% Si–3.2 wt% B (American Welding Society designation, BNi-3) droplets on NiAl substrates. The Ni–Si–B filler metal was chosen for examination because one of the present authors has previously demonstrated the applicability of this material as an interlayer for NiAl–NiAl and NiAl–Ni joining [10, 11].

The paper examines the influence, on wettability, of the residual oxide layer present on the surface of the NiAl substrates. The effect of the onset of isothermal solidification on spreading of the Ni–Si–B filler metal is also examined.

## 2. Experimental techniques

Investigations of the wettability of cast near-stoichiometric polycrystalline Ni–48 at% Al (hereafter called NiAl) by punched discs of 1 mm diameter and 51 μm thickness melt-spun Ni–4.5 wt% Si–3.2 wt% B foil were undertaken. The NiAl substrates were polished to a 0.1 μm alumina slurry finish. Both the NiAl substrates and the Ni–Si–B foil were ultrasonically cleaned in acetone and vacuum desiccated prior to the wettability experiments. Following the cleaning and drying treatments, selected substrates were pre-oxidized in laboratory air for either 40 or 80 min at 1300 °C.

Observation of the spreading of the Ni–Si–B filler metal on the NiAl substrates was performed dynamically using a Leitz 1750 heating stage mounted on a Leitz DMR light microscope. Hot-stage light microscopy was performed under a $2 \times 10^{-4}$ Pa vacuum atmosphere at a temperature of approximately 1150 °C. Observations were recorded on video both using conventional illumination and recording and also via a strobe source–field grabber combination.

The results of the hot-stage light microscopy studies were compared with post-spreading room-temperature scanning electron microscopy (SEM), energy-dispersive X-ray spectroscopy (EDS) and Auger electron spectroscopy (AES). SEM and EDS analysis employed a JEOL 840 microscope operated at 20 kV. EDS was performed using a Tracor–Northern 5500

0022–2461

analyser. AES was conducted using a JEOL JAMP 30 instrument.

## 3. Results and discussion

The Ni–Si–B filler-metal was able to wet both non-pre-oxidized and pre-oxidized NiAl substrates (Figs 1–3). In the case of non-pre-oxidized NiAl substrates (Fig. 1), spreading of the Ni–Si–B filler metal commenced immediately after melting (defined as time zero in Figs 1–3). In contrast, in the case of the pre-oxidized NiAl substrates, dewetting of the liquid Ni–Si–B filler metal (Fig. 4) was observed initially (producing the decrease in droplet diameter shown in Figs 2 and 3). This initial dewetting stage was subsequently followed by spreading of the Ni–Si–B filler metal. An initial (pre-melting) filler metal diameter of 1 mm was employed in all cases. The brief decrease in projected diameter observed in Fig. 1 was the result of droplet shape changes *during* melting and should not be confused with the prolonged dewetting *after* melting observed in Figs 2 and 3.

In the case of both the non-pre-oxidized and the pre-oxidized substrates, spreading gradually ceased

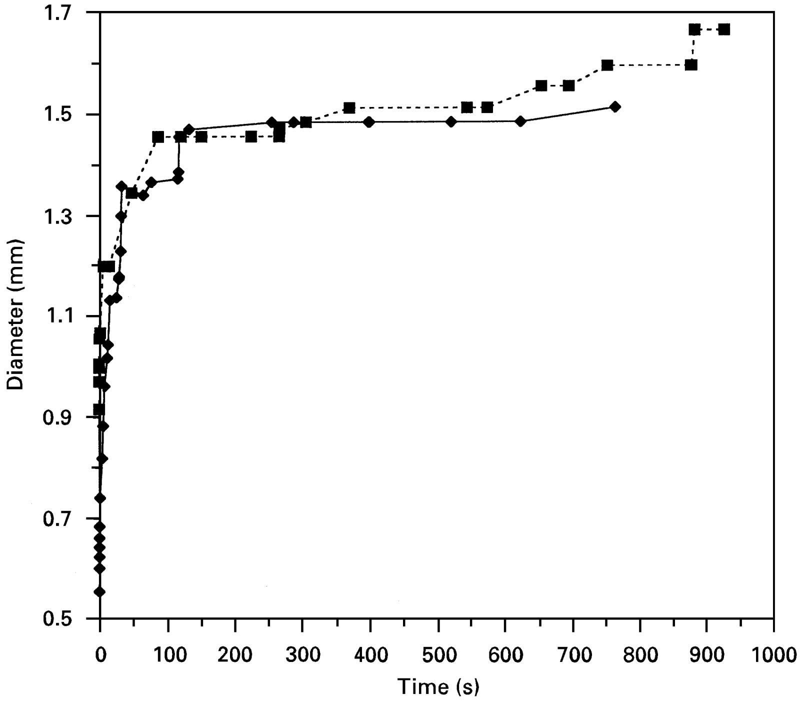

*Figure 1* Ni–Si–B droplet diameter, on a non-pre-oxidized NiAl substrate, as a function of holding time at 1150 °C. (—◆—), run A; ( – – –■– – – ), run B.

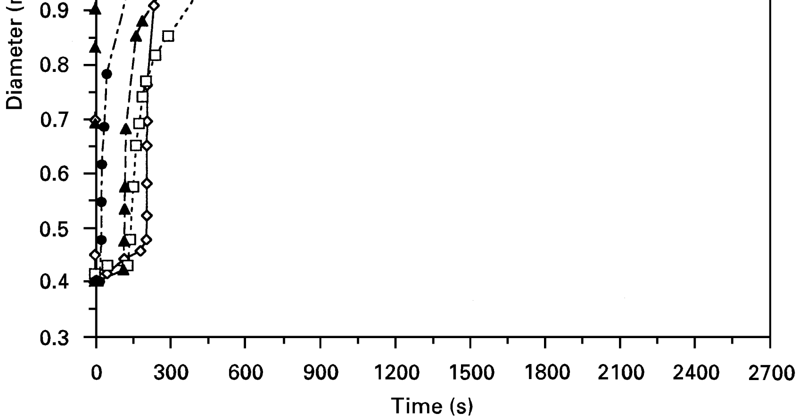

*Figure 2* Ni–Si–B droplet diameter, on an NiAl substrate pre-oxidized for 40 min at 1300 °C, as a function of holding time at 1150 °C. ( —◇— ), run C; ( – – –□– – – ), run D; (— –▲– —), run E; ( — - —●— - — ), run F.

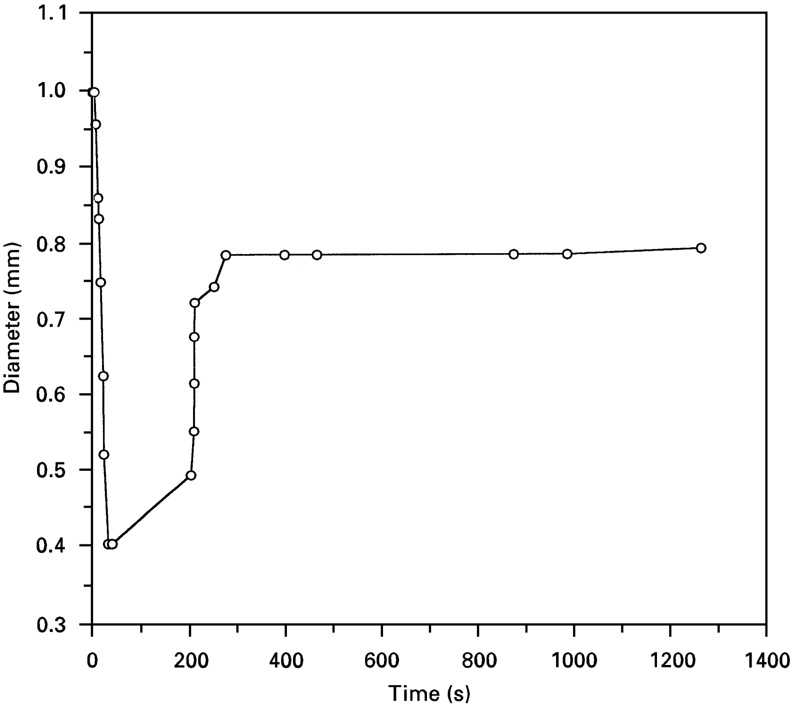

*Figure 3* Ni–Si–B droplet diameter, on an NiAl substrate pre-oxidized for 80 minutes at 1300 °C, as a function of holding time at 1150 °C. ( —O— ), run G.

with increasing holding time at 1150 °C (as can be seen in Figs 1–3). Significant scatter was observed between runs for a given substrate condition. Nonetheless, a general tendency was observed for a reduced terminal extent of spreading on progressing from non-pre-oxidized substrates (runs A and B in Fig. 1) via pre-oxidation for 40 min at 1300 °C (runs C–F in Fig. 2) to pre-oxidation for 80 min at 1300 °C (run G in Fig. 3).

In this section, the influence of isothermal solidification of the filler metal, and the oxide layer present on the NiAl substrates on the wettability of NiAl by Ni–Si–B is examined. Comparisons are drawn between the present investigation of the NiAl/(Ni–Si–B) system and previous work by one of the present authors on the wettability of nickel-based alloys by liquid Ni–Si–B.

## 3.1. Undermining of the substrate oxide layer

In many systems (see, for example, [14–16]), spreading of liquid metals on the surface of oxidized metallic substrates occurs by propagation of the liquid along the substrate metal–substrate oxide interfaces (i.e., the substrate oxide is "undermined" by the spreading liquid). In the present case of Ni–Si–B liquids spreading on NiAl substrates, evidence was obtained from post-spreading SEM and EDS investigations that the filler metal spread by undermining of the substrate oxide on non-pre-oxidized NiAl substrates. In these SEM and EDS investigations (Fig. 5) the lifting by the Ni–Si–B filler metal of an aluminium-rich layer (presumably alumina) originally present on the surface of the NiAl substrates was clearly observable. In the case of NiAl substrates pre-oxidized for 40 or 80 min at 1300 °C, the undermining of the substrate oxide layer by the liquid Ni–Si–B filler metal could be observed directly in the hot-stage light microscope.

In previous work by one of the present authors, on spreading of Ni–P, Ni–Pd–Si and Cu droplets (similar behaviour was not observed for Ni–Si–B droplets which reduced rather than undermined the oxide on Ni–Cr substrates [17]) on Ni(–Cr) substrates [18], the substrate-oxide-undermining process was found to occur in a stepwise fashion. In these systems, rapid bursts of spreading were separated by protracted holding periods (lasting up to 100 s) in which the main spreading front remained stationary. The holding periods were observed to commence when the spreading front impinged on shear cracks in the substrate oxide, which were present above substrate grain boundaries. During the holding periods, whilst the main liquid front was stationary, spreading continued in thin streams along those substrate grain boundaries surmounted by shear cracks in the substrate oxide. In order to explain these observations, one of the present authors and a co-worker [18] proposed a mechanism in which propagation of the main liquid front and spreading along substrate grain boundaries occur in competition. In this mechanism, the following events take place.

1. Spreading along and into the substrate grain boundaries (the grain-boundary mode of spreading actually consists of a combination of two processes, namely spreading along the bare metal surface at the base of the cracks in the oxide above substrate grain boundaries, and spreading down into the grain boundaries) results initially in a greater rate of interfacial energy release than propagation of the main liquid front by undermining of the substrate oxide. Hence, on first reaching a grain boundary surmounted by cracked oxide, spreading of the main liquid front

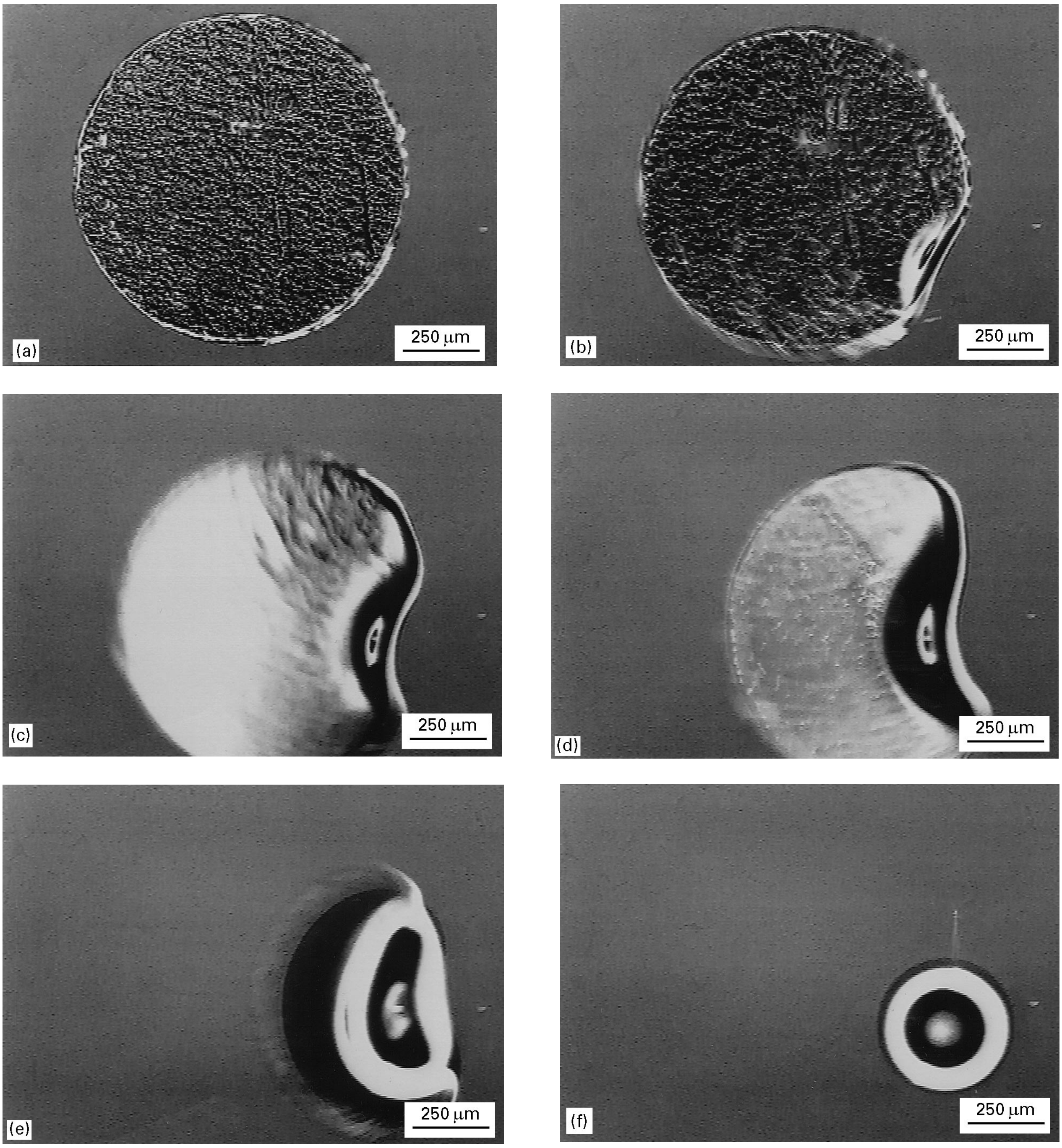

*Figure 4* Hot-stage light microscope video stills showing dewetting, after melting, of an Ni–Si–B droplet on an NiAl substrate pre-oxidized for 40 min at 1300 °C: (a) 0 ms; (b) 420 ms; (c) 490 ms; (d) 560 ms; (e) 630 ms; (f) 700 ms.

ceases and spreading instead continues along the boundary.

2. Interdiffusion between the filler metal and the substrate changes the composition of the thin stream of filler metal spreading along and into substrate grain boundaries more rapidly than for the main liquid front.

3. The changes in composition of the stream of filler metal spreading along and into substrate grain boundaries gradually make the spreading of this stream sufficiently sluggish for propagation of the main liquid front to produce a greater rate of interfacial energy release. At this point, propagation of the main liquid front recommences.

The initial rate of interfacial energy release resulting from spreading along oxide-covered substrate grain boundaries was modelled [18] as being lower than in the case of substrate grain boundaries surmounted by cracked oxide. Reductions in the rate of interfacial energy release, due to increasingly sluggish spreading resulting from interdiffusion with the substrate, would occur regardless of the continuity of the substrate oxide. However, these reductions have a more significant effect in the case of the continuous oxide than the cracked oxide because of the smaller initial rate of interfacial energy release in the former case than the latter.

It was observed experimentally [18], in the case of Ni–P spreading on Ni(–Cr) substrates, that preferential spreading along substrate grain boundaries was much less protracted in the case of a continuous

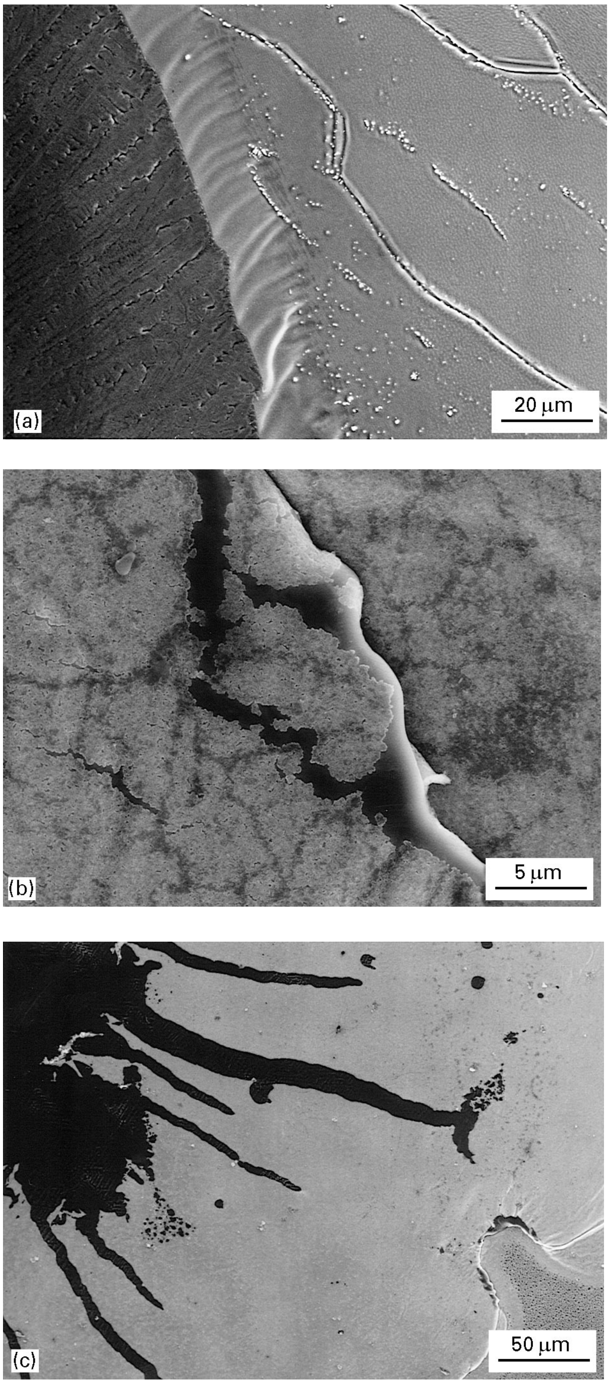

*Figure 5* Secondary-electron images showing undermining of the NiAl substrate oxide layer by the Ni–Si–B filler metal (the filler metal is dark, and the substrate oxide light): (a) non-pre-oxidized substrate; (b), (c) substrate pre-oxidized for 40 min at 1300 °C.

substrate oxide than for substrate oxide with cracks about the substrate grain boundaries. Thus, when the oxide layer above the substrate grain boundaries was continuous (as, for example, in the case of a pre-oxidized substrate), propagation of the main liquid front occurred almost continuously and stepwise spreading did not occur. The significance of these observations was that, counterintuitively, the presence of discontinuities in the substrate oxide hindered rather than aided the spreading process.

In the present case of the NiAl/(Ni–Si–B) system (with or without a pre-oxidation treatment), preferential spreading along substrate grain boundaries was observed to be much less important than in the case of Ni–P, Cu or Ni–Pd–Si spreading on Ni(–Cr) substrates. Preferential spreading along substrate grain boundaries only occurred (after the onset of isothermal solidification at the edge of the spreading droplets) at the initiation of localized "overflowing" events (discussed in Section 3.3). Furthermore, even when spreading did occur along substrate grain boundaries, this was followed after less than 1 s by spreading over the substrate grain interiors. Thus, spreading of the Ni–Si–B liquid on the NiAl substrates generally occurred in a continuous rather than a stepwise fashion (as can be seen from the relatively smooth droplet diameter versus time curves shown in Figs 1–3).

When the condition of the NiAl substrate oxide layer was examined by post-spreading SEM, the oxide layer (on both pre-oxidized and non-pre-oxidized substrates) was found to form a continuum across substrate grain boundaries. Hence, the spreading behaviour observed in the NiAl/(Ni–Si–B) system supports the model developed previously for Ni–Cr substrates. Indeed, even in the case of pre-oxidized substrates, once spreading was initiated, the Ni–Si–B filler metal spread readily by undermining of the oxide layer on the NiAl substrates.

A potential source of confusion, in examining the role of substrate grain boundaries in the spreading process, is the occurrence of thermal grooving of the substrate grain boundaries, during high-temperature wettability experiments. These thermal grooves provide fine capillary paths and hence possible sites for preferential spreading. In the present investigation of NiAl substrates, grooving of the substrate grain boundaries was observed. However, the aluminium-rich (presumably alumina) surface layer remained continuous over the grooved substrate grain boundaries. In the present investigation, the occurrence of these grooves, without substrate oxide discontinuities, was not found to result in significant preferential spreading along the substrate grain boundaries.

## 3.2. Interfacial reactions

### 3.2.1. *Phenomena*

As was discussed in Section 3.1, post-spreading SEM and EDS (on samples that had not received a substrate pre-oxidation treatment) revealed the presence of an aluminium-rich layer (presumably alumina), over outer regions of the spread filler. This layer was lifted from the NiAl substrate by the spreading Ni–Si–B filler. In general, the layer was undamaged by the lifting process, although rumpling of the layer during lifting was observed in some locations. However, this continuous aluminium-rich layer was not detectable over the bulk surface of the spread droplet behind the spreading front, even after large extents of spreading.

The presence of aluminium- and silicon-rich particles was observed in the aluminium-rich layer immediately ahead of the spreading Ni–Si–B droplet. The presence of these particles is consistent with the formation of either an aluminosilicate and/or an aluminoborosilicate (the EDS detector employed will not detect either oxygen or boron). It is unlikely that the particles are borides, as nickel, rather than aluminium or silicon, is the major metallic constituent of the $M_{23}B_6$ and $M_3B$-type borides formed in NiAl/(Ni–Si–B) TLP bonds [10, 11].

It was noted in Section 3.1 that, in the case of substrates subjected to a pre-oxidation treatment, consisting of 40 or 80 min exposure to 1300 °C laboratory air, the oxide was clearly visible using light microscopy. Hence, in these samples, the undermining of the substrate oxide by the filler metal was observable directly in the hot-stage light microscope. However, surprisingly, the oxide from the substrate oxide layer carried up onto the spreading Ni–Si–B droplet by the spreading process gradually "disappeared" behind the spreading front (Fig. 6). At first, this disappearance was localized, with holes formed in the lifted substrate oxide layer behind the spreading front (these holes remained present after cooling). However, with continued holding at 1150 °C, the apparent loss of the lifted oxide became generalized.

The density of a solid alumina scale would be expected to be lower than that of liquid Ni–Si–B. Thus, solid alumina should float on the surface of the liquid Ni–Si–B and indeed this was generally observed. Furthermore, in the absence of a marked reaction at the oxide–liquid metal interface, metal oxides are not wettable by liquid metals [19]. Moreover, if the substrate oxide was wettable by the liquid, then spreading of the liquid could take place along the outer surface of the oxide, rather than by undermining. In some regions of the spreading front, the substrate oxide was fragmented (during undermining of the alumina layer) and became temporarily entrained in the spreading liquid. However, this oxide subsequently floated up to the surface of the liquid droplet. Over most of the spreading front, alumina was carried initially more or less intact onto the surface of the alumina droplet. Thus, the apparent disappearance of the oxide does not seem to have resulted from submersion of the oxide layer in the liquid filler metal.

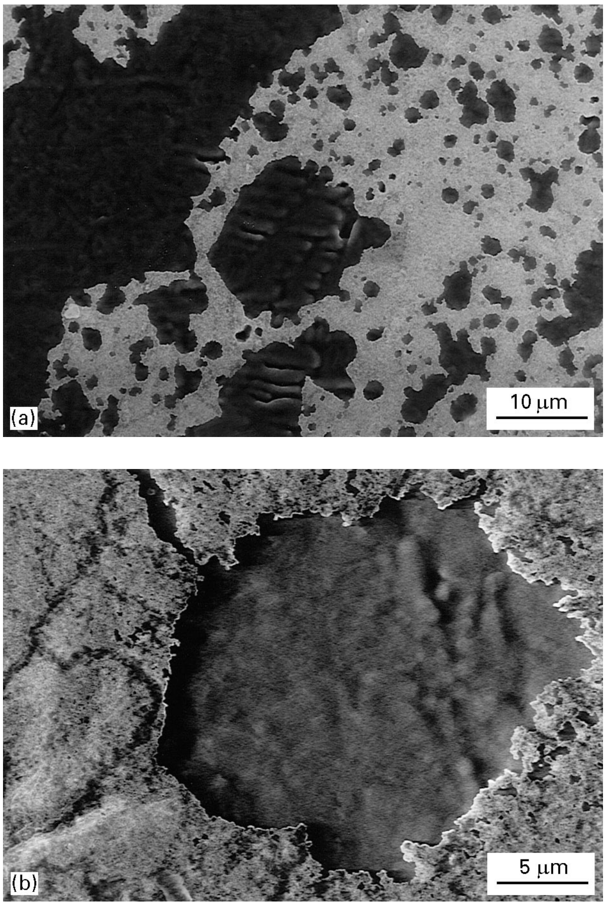

*Figure 6* Secondary-electron images showing degradation of the substrate oxide layer on an NiAl substrate, pre-oxidized for 40 min at 1300 °C, after lifting onto the Ni–Si–B filler metal droplet (the filler metal is dark, and the lifted substrate oxide light): (a) overview; (b) detail.

In searching for an explanation for the apparent disappearance of the substrate oxide layer after undermining by the liquid filler, the possibility of a reaction between the liquid droplet and the substrate oxide must be considered. Whereas boron emanating from the filler metal has been observed to reduce the oxide layers present on Ni–Cr substrates [17], alumina is not reducible by either filler metal boron or silicon. However, a reaction between the filler-metal oxide and the substrate oxide is possible and this reaction is discussed in the next section.

The apparent "disappearance" of the oxide layer on pre-oxidized NiAl substrates, after lifting by the spreading filler-metal raises two issues, namely the nature of the process giving rise to the apparent disappearance of the substrate oxide and the role of this oxide disappearance process in spreading of the Ni–Si–B filler metal. These two issues are discussed in the remainder of this section. The thermodynamics of possible reactions between the filler metal and the substrate oxide is first examined. Subsequently, experimental observations of the spreading droplets are discussed.

### 3.2.2. *Thermodynamic analysis*

As shown in the Ellingham diagram (drawn using data from [20, 21] and assuming ideal solutions) in Fig. 7, $Al_2O_3$ is more stable than NiO, $SiO_2$ or $B_2O_3$ and thus should not be reduced by a Ni–4.5 wt% Si–3.2 wt% B alloy. However, $Al_2O_3$ could dissolve in an oxide which may form from reaction of filler metal constituents with residual oxygen in the vacuum chamber atmosphere. Fig. 7 shows that $SiO_2$ and $B_2O_3$ are much more stable than NiO, even considering the reduced activities of B and Si in the alloy. Hence, the oxide formed on the Ni–Si–B alloy would most probably be a borosilicate.

*3.2.2.1. Formation of a liquid borosilicate.* At high oxygen partial pressures, a protective silica layer is formed on silicon (i.e., passive oxidation), whilst at low oxygen partial pressures a non-protective gaseous reaction product, SiO, forms (i.e., active oxidation). The critical oxygen partial pressure for the transition between passive and active oxidation, $p^*_{O_2}$, is related to the equilibrium SiO(g) pressure, $p^{equ}_{SiO}$, for the reaction

$$SiO_2(s) + Si(s) = 2SiO(g) \qquad (1)$$

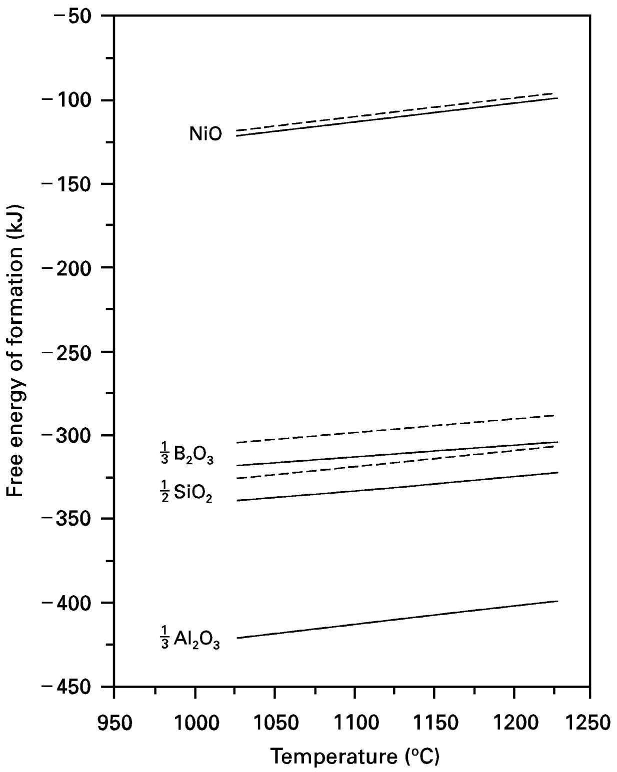

*Figure 7* Gibb's free energy of formation of NiO [20], $B_2O_3$ [21], $SiO_2$ [21] and $Al_2O_3$ [21]. (——), unit metal activities; (– – –), $a_B = 0.15$, $a_{Si} = 0.08$ and $a_{Ni} = 0.77$.

according to

$$p^*_{O_2} = \frac{1}{2}\left(\frac{D_{SiO}}{D_{O_2}}\right)^{1/2} p^{equ}_{SiO} \qquad (2)$$

where $D_{SiO}/D_{O_2}$ is the ratio of the diffusivity of SiO(g) to the diffusivity of $O_2$(g) and is estimated to be 0.64 [22].

The critical oxygen partial pressure for an alloy with a silicon activity of 0.08 at 1150 °C is approximately $4 \times 10^{-5}$ Pa [20]. If the residual atmosphere in the vacuum is air (21% oxygen), then the oxygen partial pressure in the vacuum chamber is $4 \times 10^{-5}$ Pa. Thus, the atmosphere in the vacuum chamber is at the critical oxygen partial pressure for the formation of silica.

The $BO_x$ gas species with the highest equilibrium partial pressure under the present experimental conditions is $B_2O_3$(g). Although water vapour can increase the vaporization rate of $B_2O_3$ owing to the formation of $HBO_2$ or $H_3BO_3$ [23], the equilibrium partial pressures of these B–H–O gas species, using the maximum possible water vapour partial pressure (i.e. the total vacuum pressure), are lower than that of $B_2O_3$(g). The equilibrium partial pressure of $B_2O_3$(g) at 1150 °C is $5 \times 10^{-4}$ Pa, which slightly exceeds the vacuum pressure ($2 \times 10^{-4}$ Pa) and so any liquid $B_2O_3$ formed would be expected to vaporize. However, the presence of $SiO_2$ could result in the formation of a borosilicate and this would reduce the activity of $B_2O_3$ to below unity. The reduced $B_2O_3$ activity may, in turn, reduce the $B_2O_3$ vapour pressure to a level below the vacuum pressure and thus reduce the vaporization rate of $B_2O_3$.

The solubility of $B_2O_3$ in solid $SiO_2$ is limited and hence, since the $SiO_2$–$B_2O_3$ eutectic temperature is 372 °C, even small $B_2O_3$ additions will result in the formation of a two-phase mixture of solid $SiO_2$ and liquid borosilicate at 1150 °C. The liquidus $SiO_2$–$B_2O_3$ composition at 1150 °C contains 15 mol% $B_2O_3$ and therefore any borosilicate containing more than 15 mol% $B_2O_3$ will be completely liquid [24]. The formation of a liquid borosilicate–solid alumina interface will provide good contact for reaction between the two phases.

*3.2.2.2. Solubility of $Al_2O_3$ in a liquid borosilicate.* At 1150 °C, the solubility of $Al_2O_3$ in pure solid $SiO_2$ is negligible, whilst 10 mol% $Al_2O_3$ can dissolve in liquid $B_2O_3$ [24]. According to the liquidus projections in the $Al_2O_3$–$SiO_2$–$B_2O_3$ ternary phase diagram, the solubility of $Al_2O_3$ in a borosilicate melt decreases with increasing silica content [24]. However, even for a relatively high $SiO_2$ concentration, 66.7 mol% $SiO_2$, approximately 3 mol% $Al_2O_3$ can dissolve in a borosilicate melt at 1150 °C [24].

The composition of the borosilicate melt may change with time at 1150 °C. The boron oxide concentration is likely to decrease with increasing holding time at 1150 °C, owing to vaporization of $B_2O_3$ and/or diffusion of boron into the NiAl substrate. As the boron oxide concentration in the borosilicate decreases, the solubility of $Al_2O_3$ also decreases and so the borosilicate may become supersaturated with $Al_2O_3$. According to the $Al_2O_3$–$SiO_2$–$B_2O_3$ ternary phase diagram, the mullite solid solution between $9Al_2O_3 : 2B_2O_3$ and $3Al_2O_3 : 3SiO_2$ is the stable solid phase in equilibrium with a borosilicate melt [24]. Thus, vaporization of $B_2O_3$ may result in the precipitation of mullite when the solubility limit of $Al_2O_3$ in the liquid borosilicate is exceeded.

### 3.2.3. Experimental support for a substrate oxide dissolution process

An attempt was made to confirm the conclusions of the thermodynamic analysis using AES depth profiling at the edge of a Ni–Si–B droplet on a preoxidized (40 min at 1300 °C) NiAl substrate. Rumpling of the substrate oxide layer occurred as this layer was lifted off the substrate and onto the spreading droplet. This rumpling, in turn, had the effect of increasing the thickness of alumina that had to be removed by sputtering before the interface between the spreading droplet and the lifted oxide could be analysed. Unfortunately, by the time that the lifted oxide was sputtered through, sufficient ion beam mixing had occurred so that distinct microstructural layers could not be identified. Thus, it was not possible to determine the composition of the interface between the lifted oxide and the spreading droplet.

A key observation, in support of the occurrence of a solutioning-type reaction (as hypothesized in Section 3.2.2) was the occurrence of a precipitation process above the centre of the spread droplet. This precipitation process was observed as a part of the following sequence of events.

1. The substrate oxide was lifted onto the oxide (with significant cracking and rumpling at the edge of the droplet).

2. Pieces of substrate oxide that cracked off the main lifted layer were carried away onto the droplet centre where they appeared to gradually dissolve.

3. The main substrate oxide layer gradually dissolved.

4. After holding for around 20–25 min at 1150 °C, precipitates appeared on the surface of the liquid droplet. The liquid droplet dewetted away from these precipitates. Increasing the holding temperature to around 1200 °C had the effect of re-solutioning these precipitates. Following holding for a further 5–10 min at 1200 °C, the precipitates began to re-form. Increasing the temperature further continued the cycle of re-solutioning and re-precipitation. These precipitates were not readily distinguishable on the irregular surface of the resolidified Ni–Si–B droplet after cooling to room temperature. However, as was noted in Section 3.2.1, aluminium- and silicon-rich precipitates (consistent with the formation of an aluminosilicate and/or aluminoborosilicate) were observed in the substrate oxide layer surrounding the Ni–Si–B droplet of a non-pre-oxidized substrate.

This sequence of events is entirely consistent with dissolution of the substrate alumina layer in a liquid borosilicate layer on the Ni–Si–B droplet's surface, followed by supersaturation of the borosilicate with alumina (and increases in alumina solubility in the borosilicate with increasing temperature).

### 3.2.4. The role of substrate oxide–filler metal reaction in spreading

Even if the occurrence of a substrate oxide dissolution reaction is accepted, evidence is required that this reaction serves a role in the spreading of the Ni–Si–B liquid. Possible roles of substrate oxide dissolution in the spreading process will first be discussed and evidence for the occurrence of these roles will then be examined.

Encouragement of spreading of the filler metal by the substrate oxide dissolution process could take one or both of the two following forms.

1. During the initiation of spreading, the filler metal must pass from the substrate oxide–atmosphere interface, through defects (pores or cracks) in the oxide, to the substrate metal–substrate oxide interface. Thus, given a finite oxide thickness, the filler metal must be able to spread down the sides of the oxide defect (at least to some extent) if spreading is to be initiated. Alumina is non-wettable by the Ni–Si–B filler metal (e.g., the Ni–Si–B filler forms spherical non-wetted droplets on a bulk alumina substrate). Hence, the occurrence of a spreading-promoting substrate oxide dissolution process could contribute strongly to allowing the filler metal to pass down through defects in the substrate oxide (i.e., such a dissolution reaction would aid the initiation of spreading).

2. Once the filler metal has reached the substrate oxide–substrate metal interface, a dissolution process that increases the driving force for spreading might contribute to the propagation of spreading. A thermodynamically favourable substrate oxide dissolution reaction would, in turn, provide a driving force for expansion of the area over which the reaction was occurring [25]. Such an expansion in the reacting area would presumably require an expansion in the substrate oxide–filler metal interfacial area. Hence, as in the case of direct reactions between filler metal constituents and the substrate [25], the presence of the dissolution reaction would encourage spreading of the filler metal.

Furthermore, a substrate oxide dissolution process could aid *directly* in the propagation of substrate oxide undermining. Wall and Milner [14] suggested that dissolution of the substrate metal in the filler metal aids in decohesion of the oxide layer from the substrate. Conceivably, partial dissolution of the substrate oxide could have a similar effect (on decohesion of the substrate oxide from the substrate metal) to dissolution of the substrate metal.

It was noted experimentally that the initiation of spreading on pre-oxidized NiAl substrates occurred significantly after melting of the Ni–Si–B filler metal. Immediately after melting, the filler metal disc formed a non-wetting spherical globule. Approximately 1–3 min after melting, a darkened halo was observed on the substrate oxide surrounding the Ni–Si–B globule. Around 10–30 s after the first observation of this halo, rapid spreading of the Ni–Si–B droplet was initiated. Subsequent to the initiation of spreading, the darkened halo grew ahead of the spreading front. These observations are consistent with and suggestive of initiation of spreading by a reaction between a reagent associated with the filler metal and the substrate oxide. Indeed, in the case of some punched foil discs for which only some regions made close contact with the substrate before melting, the apparent occurrence of a reaction between a reagent associated with the filler metal and the substrate oxide could be discerned prior to melting. In these samples, the formation of a series of interference fringes, concentric with the point (or points) of contact between the filler metal and the substrate, was observed at temperatures of approximately 800 to 900 °C and above. The formation of the interference fringes is indicative of removal of the substrate oxide.

With regard to the possible role of solutioning of alumina in the (liquid) oxide formed on the filler in the *propagation* of spreading, a significant observation was made using post-spreading SEM. In this SEM work, it was observed that, in the case of some NiAl substrates which produced alumina layers with significant porosity, sintering of these pores occurred ahead of the spreading droplet (Fig. 8). The sintered region formed a halo around the droplet with a width of approximately 10 μm. In searching for an agent capable of sintering the pores in the alumina, liquid $B_2O_3$ (or a borosilicate) emanating from the oxide layer on the filler metal appears the most likely candidate. If sintering occurred ahead of the droplet, then the sintering agent must be transported ahead of the droplet. Hence, it would appear that, if $B_2O_3$ (or

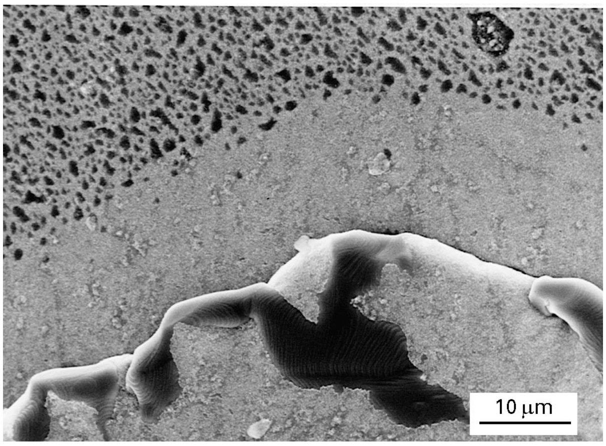

*Figure 8* Secondary electron image showing sintering of the oxide layer on an NiAl substrate, pre-oxidized for 40 min at 1300 °C (the bulk substrate oxide is at the top, the sintered substrate oxide in the middle, and the filler metal at the bottom).

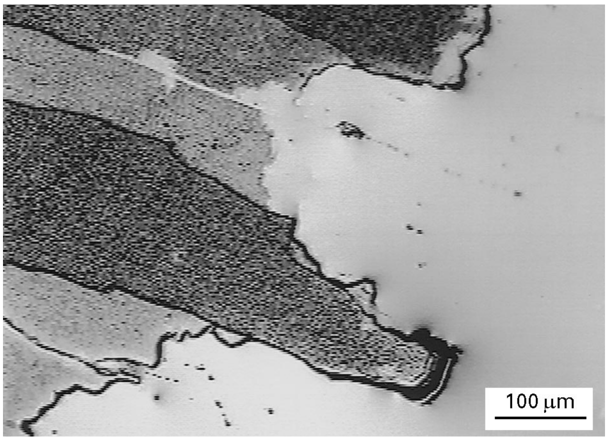

*Figure 9* Hot-stage light microscope video still showing residual spreading after the onset of isothermal solidification at the edge of a Ni–Si–B droplet on a non-pre-oxidized NiAl substrate (the filler metal is light, and the substrate dark).

a borosilicate) was indeed the sintering agent, then $B_2O_3$ (or a borosilicate) would have been available at (and ahead of) the spreading front to influence the propagation of spreading of the Ni–Si–B droplets.

## 3.3. Isothermal solidification

Spreading of the Ni–Si–B filler metal on the NiAl substrates was observed to occur rapidly and uniformly until the initiation of isothermal solidification at the spreading front. Once isothermal solidification commenced at the edge of the droplet, however, spreading was found to cease gradually. Spreading after the onset of isothermal solidification generally occurred by a slow uniform flowing of the remaining liquid over the band of isothermally re-solidified filter metal at the outer extremities of the Ni–Si–B droplet. In contrast, sudden bursts of spreading (Fig. 9) due to localized overflowing of the isothermally re-solidified filler by the residual liquid were both relatively rare and short lived when compared with similar events during the spreading of the Ni–Si–B filler on Ni(–Cr) substrates [17]. The origins of this difference are uncertain and require further investigation.

Dissolution of the NiAl substrate into the Ni–Si–B filler metal and silicon diffusion from the filler into the NiAl substrates were slight after the durations (up to 45 min at 1150 °C) examined in the present work (and this matches observations in bulk TLP bonds [11]). Thus, the major factor leading to the onset of isothermal solidification of the Ni–Si–B droplets was presumably loss of boron from the filler metal.

In previous work by one of the present authors and a co-worker [17] concerning Ni–Si–B droplets spreading on Ni(–Cr) substrates, removal of boron from the liquid droplet (and hence the initiation of isothermal solidification) occurred primarily by reaction of boron with the lifted substrate oxide layer, rather than by boron diffusion into the bulk substrate. In contrast, in the present work on spreading of Ni–Si–B on NiAl substrates, a *direct* reaction is not expected between boron (initially in solution in the liquid filler) and the substrate (alumina) oxide layer. Instead, a reaction between $B_2O_3$ *pre-existing* on the surface liquid filler at the time of reaction and the substrate oxide has been hypothesized.

A reaction between a pre-existing $B_2O_3$ layer and the substrate oxide would not deplete boron from the liquid filler metal and hence would not be expected to contribute to the onset of isothermal solidification of the liquid filler metal. Indeed, it was observed experimentally that Ni–Si–B droplets spreading on non-pre-oxidized, lightly pre-oxidized and heavily pre-oxidized substrates all commenced isothermal solidification within the same time frame (typically 30–180 s holding at 1150 °C) after the initiation of spreading. Thus, it may be assumed, in the NiAl/(Ni–Si–B) system, that the onset of isothermal solidification occurred entirely as a result of interdiffusion between the filler metal and the substrate. One of the present authors and co-workers [26] has estimated the boron diffusivity in NiAl (at a temperature of 1150 °C) to be around $10^{-12}\,\mathrm{m^2\,s^{-1}}$. This relatively low boron diffusivity, together with the absence of boron depletion from the filler by *direct* reaction with the substrate oxide, would account for the relatively slow onset of isothermal solidification at the edge of the Ni–Si–B droplets (approximately 30–80 s holding at 1150 °C, after the start of spreading was required to initiate observable isothermal solidification at the edges of the filler metal droplets compared with a few seconds for similar droplets spreading on Ni–Cr substrates [17]).

## 4. Conclusions

An investigation has been undertaken of the wettability of NiAl by a liquid Ni–4.5 wt% Si–3.2 wt% B alloy. As a result of this investigation, the following conclusions have been drawn.

1. Spreading of the Ni–Si–B filler on NiAl substrates occurred by undermining of the substrate oxide layer by the filler metal. In the presence of a continuous substrate oxide layer over substrate grain boundaries, the filler metal did not show a marked preference

for propagation along substrate grain boundaries. Thus, spreading occurred in a uniform rather than a localized stepwise fashion.

2. Thermal grooving of the NiAl substrate grain boundaries was observed. However, in the absence of discontinuities in the substrate oxide layer, this grooving did not result in preferential spreading of the filler metal along substrate grain boundaries.

3. The spreading of the Ni–Si–B filler on NiAl was consistent with a mechanism (previously proposed by one of the present authors and a co-worker) in which a dominant role is played by substrate oxide discontinuities, above substrate grain boundaries, in preferential spreading along substrate grain boundaries.

4. The substrate oxide layer in contact with the Ni–Si–B filler metal gradually "disappeared". Dissolution of the substrate oxide layer in a liquid borosilicate formed on the surface of the liquid filler metal has been proposed as a mechanism to account for the apparent disappearance of the substrate oxide.

5. The initiation of spreading of the Ni–Si–B filler metal on pre-oxidized NiAl substrates only occurred after a significant time delay, in a fashion that was consistent with the initiation of spreading by a reaction between constituents of the filler metal system (liquid filler plus filler metal oxide) and the substrate oxide layer.

6. Propagation of Ni–Si–B droplets across the oxidized surfaces of the NiAl substrates occurred under conditions consistent with a reaction between a component of the filler metal system and the substrate oxide layer, ahead of the spreading filler metal.

7. Spreading of the Ni–Si–B droplets on the NiAl substrates was essentially terminated by the onset of isothermal solidification at the spreading front. Unlike the case of Ni–Si–B droplets spreading on Ni(–Cr) substrates, isothermal solidification of the filler metal appeared to be independent of reactions between the filler metal system and the substrate oxide layer.

## Acknowledgement

The authors wish to express their thanks to Dr Easo George of the Oak Ridge National Laboratory for the provision of the NiAl substrate material.

## References

1. I. BAKER and P. R. MUNROE, "High temperature aluminides and intermetallics," edited by S. H. Whang, C. T. Liu, D. P. Pope and J. O. Stiegler (Metallurgical Society of AIME, Warrendale, PA, 1990) pp. 425–52.
2. S. NAKA, M. THOMAS and T. KHAN, *Mater. Sci. Technol.* **8** (1992) 291–99.
3. J. R. STEPHENS, *Mater. Res. Soc. Symp. Proc.* **39** (1985) 381.
4. K. VEDULA, V. PATHARE, I. ASLANDIS and R. H. TITRAN, *ibid.* **39** (1985) 411.
5. K. VEDULA and J. R. STEPHENS, *ibid.* **81** (1987) 381.
6. D. M. DIMIDUK, D. B. MIRACLE and C. H. WARD, *Mater. Sci. Technol.* **8** (1992) 367.
7. D. S. DUVALL, W. A. OWCZARSKI and D. F. PAULONIS, *Weld J.* **53** (1974) 203.
8. S. GUHA, P. R. MUNROE and I. BAKER, *Mater. Res. Soc. Symp. Proc.* **133** (1989) 633.
9. J. K. DOYCHAK and T. E. MITCHELL, *ibid.* **39** (1985) 475.
10. W. F. GALE and S. V. OREL, *Metall. Mater. Trans. A* **27A** (1996) 1925.
11. W. F. GALE and S. V. OREL, *J. Mater. Sci.* **31** (1996) 345.
12. T. J. MOORE and J. M. KALINOWSKI, *Mater. Res. Soc. Symp. Proc.* **288** (1993) 1173.
13. M. J. STRUM and G. A. HENSHALL, "Advanced joining technologies for new materials II" edited by N. F. Flore and J. O. Stiegler (American Welding Society, Miami, FL, 1994) pp. 76–88.
14. A. J. WALL and D. R. MILNER, *J. Inst. Metals* **90** (1961) 394.
15. J. C. AMBROSE, M. J. NICHOLAS, N. YOUNG and S. L. JENKINS, *Mater. Sci. Technol.* **6** (1990) 1021.
16. K. A. THORSEN, H. FORDSMAND and P. L. PRAESTGAARD, *Weld. J.* (*Res. Suppl.*) **63** (1984) 339s.
17. W. F. GALE and E. R. WALLACH, *J. Mater. Sci.* **27** (1992) 5653.
18. *Idem., ibid.* **28** (1993) 243.
19. G. SHEWARD, "High temperature brazing in controlled atmospheres" (Pergamon, Oxford 1985).
20. M. W. CHASE, C. A. DAVIES, J. R. DOWNEY, D. J. FRURIP, R. A. McDONALD and A. N. SYVERUD, "JANAF thermochemical tables", 3rd Edn, *J. Phys. Chem. Ref. Data* **14** (1985) Suppl. 1.
21. O. KUBASCHEWSKI and C. B. ALCOCK, "Metallurgical thermochemistry", (Pergamon, Oxford, 1979).
22. C. WAGNER, *J. Appl. Phys.* **29** (1958) 1295.
23. D. W. McKEE, *Carbon* **24** (1986) 737.
24. R. S. ROTH, J. R. DENNIS and H. F. McMURDIE, "Phase diagrams for ceramists, Vol. VI (American Ceramic Society, Westerville, OH, 1987).
25. I. A. AKSAY, C. E. HOGE and J. A. PASK, *J. Phys. Chem.* **78** (1974) 1178.
26. S. V. OREL, L. PAROUS and W. F. GALE, *Weld. J.* (*Res. Suppl.*) **74** (1995) 319s.

*Received 8 January 1996*
*and accepted 10 March 1997*